Tropical upper tropospheric temperature

GCC lecture, University of Hamburg
Hauke Schmidt & Bjorn Stevens
November 5 & 12, 2019

Discrepancy in models and observations according to IPCC AR5

„In summary, most, though not all, CMIP3 and CMIP5 models overestimate the observed warming trend in the tropical troposphere during the satellite period 1979–2012. Roughly one-half to two-thirds of this difference from the observed trend is due to an overestimate of the SST trend, which is propagated upward because models attempt to maintain static stability. There is low confidence in these assessments, however, due to the low confidence in observed tropical tropospheric trend rates and vertical structure (Section 2.4.4).“

(IPCC AR5, WG1, Section 9.4.1.4.2, Flato et al., 2013)

Model projections of zonal mean tropospheric temperature change

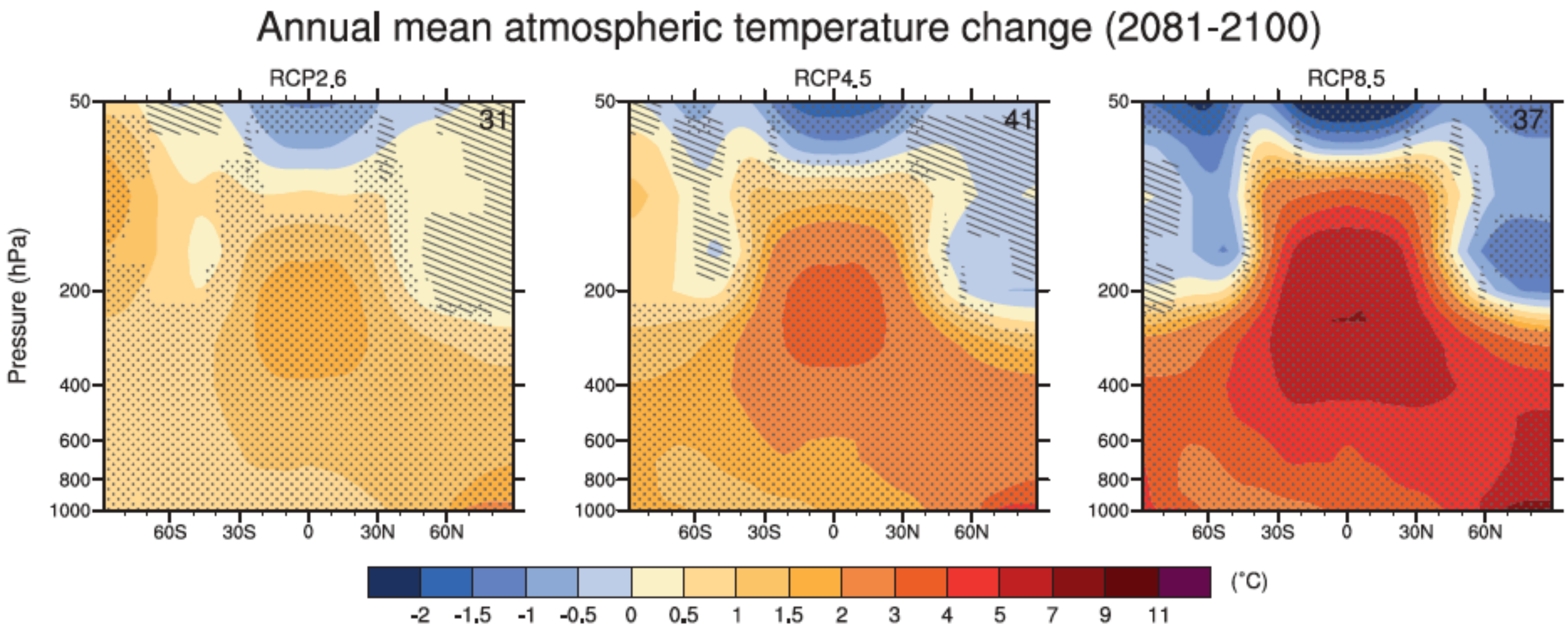

Figure 12.12 | CMIP5 multi-model changes in annual mean zonal mean temperature in the atmosphere and ocean relative to 1986–2005 for 2081–2100 under the RCP2.6 (left), RCP4.5 (centre) and RCP8.5 (right) forcing scenarios. Hatching indicates regions where the multi-model mean change is less than one standard deviation of internal variability. Stippling indicates regions where the multi-model change mean is greater than two standard deviations of internal variability and where at least 90% of the models agree on the sign of change (see Box 12.1).

(IPCC AR5, WG1, Fig. 12.12, Flato et al., 2013)

Lapse rate profile changes in CMIP3 models and a cloud resolving model

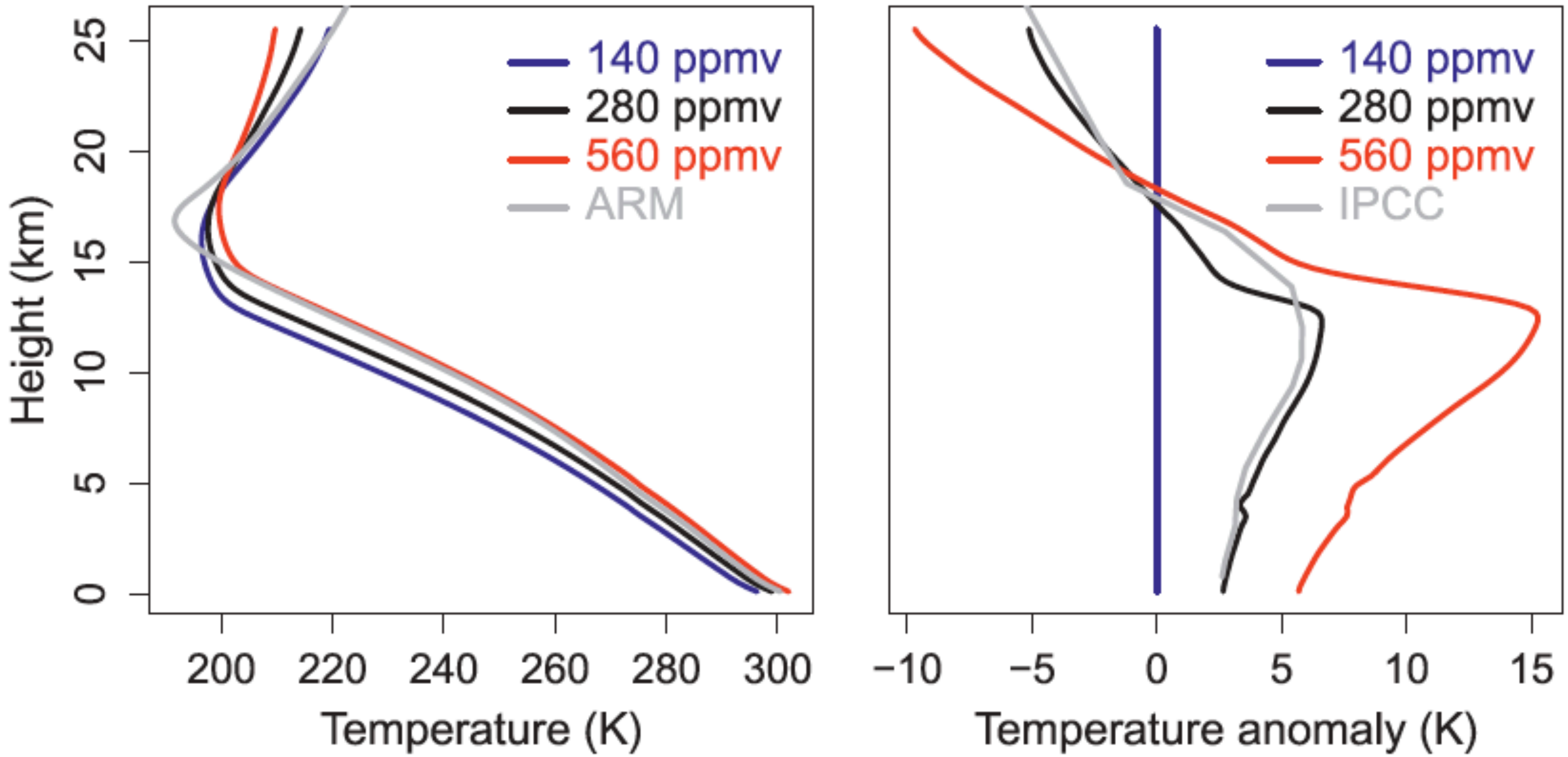

(Romps, JAS, 2011)

Discrepancy between CMIP models and radiosondes

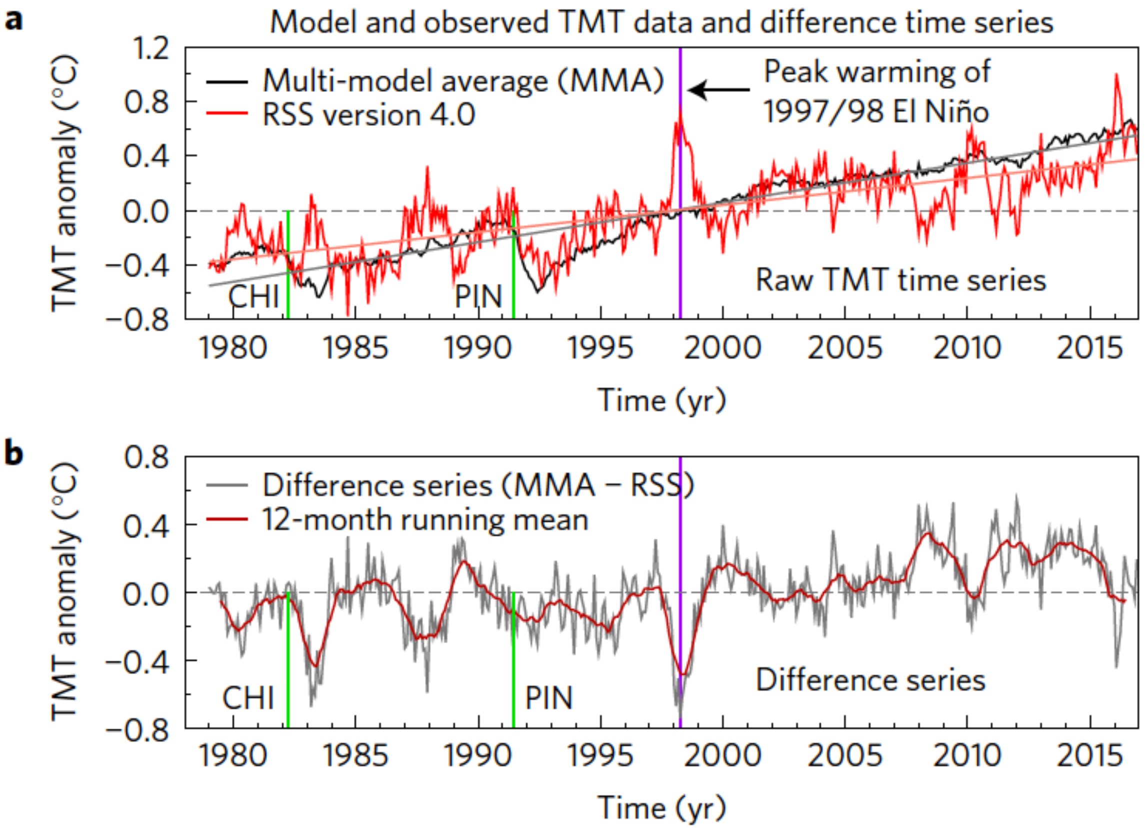

Figure 1 | Time series and difference series of simulated and observed tropospheric temperature. a, Monthly mean TMT anomalies for the 456-month period from January 1979 to December 2016, spatially averaged over 82.5° N–82.5° S and corrected for lower stratospheric cooling[40]. Multi-model average (MMA) temperature data are from HIST+8.5 simulations performed with 37 different CMIP5 models; satellite TMT data are for RSS version 4.0 (ref. 29). Model TMT data were computed using vertical weighting functions that approximate the satellite-based vertical sampling of the atmosphere[54]. **b**, Time series of differences between the MMA and the RSS data shown in both raw form and smoothed with a 12-month running mean. All anomalies are relative to climatological monthly means calculated over January 1979 to December 2016. The vertical purple line is plotted at the time of the maximum global-mean tropospheric warming during the 1997/98 El Niño. The vertical green lines denote the eruption dates of El Chichón and Pinatubo. Trends in the MMA and RSS over the full 456 months (the grey and pink lines in **a**) are 0.291 and 0.199 °C per decade, respectively. The corresponding trends over the early twenty-first century (January 2000 to December 2016) are 0.286 and 0.191 °C per decade.

Satellite IR brightness temperatures (yesterday)

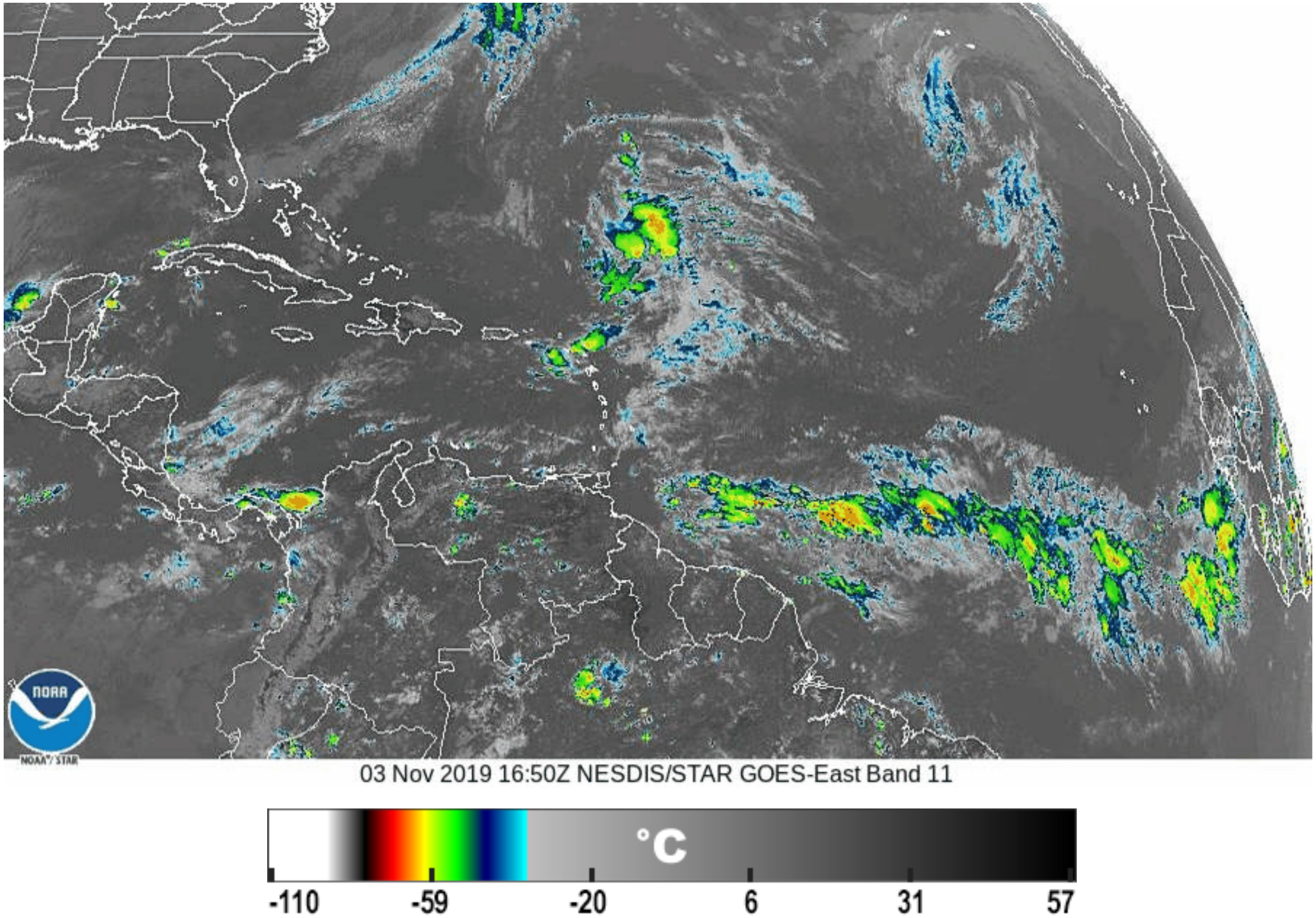

(www.star.nesdis.noaa.gov/GOES)

Tropical convective clouds

(climate.nasa.gov)

Typical tropical profiles of θ, θ_e, and θ_{es}

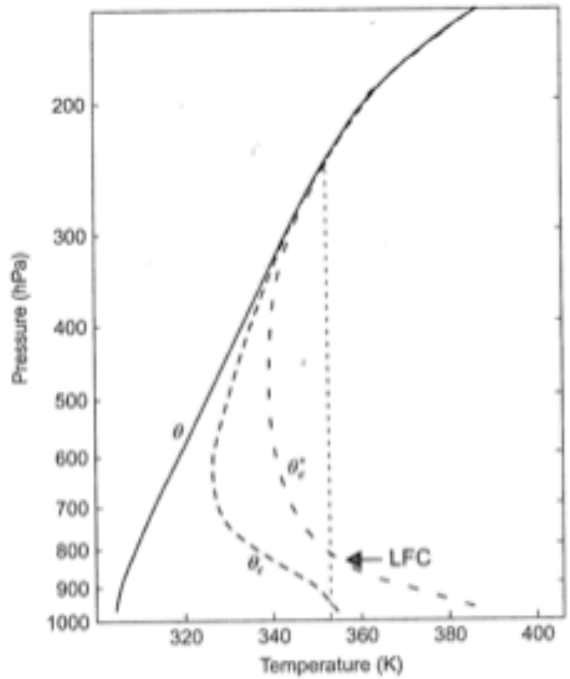

FIGURE 2.8 Schematic sounding for a conditionally unstable environment, characteristic of midwestern North American thunderstorm conditions, showing the vertical profiles of potential temperature θ, equivalent potential temperature θ_e, and equivalent temperature θ_e^* of a hypothetically saturated atmosphere with the same temperature profile. The *dotted line* shows θ_e for a nonentraining parcel raised from the surface. The *arrow* denotes the LFC for the parcel.

(Holton & Hakim, 2013)

Gravity waves resulting from convection

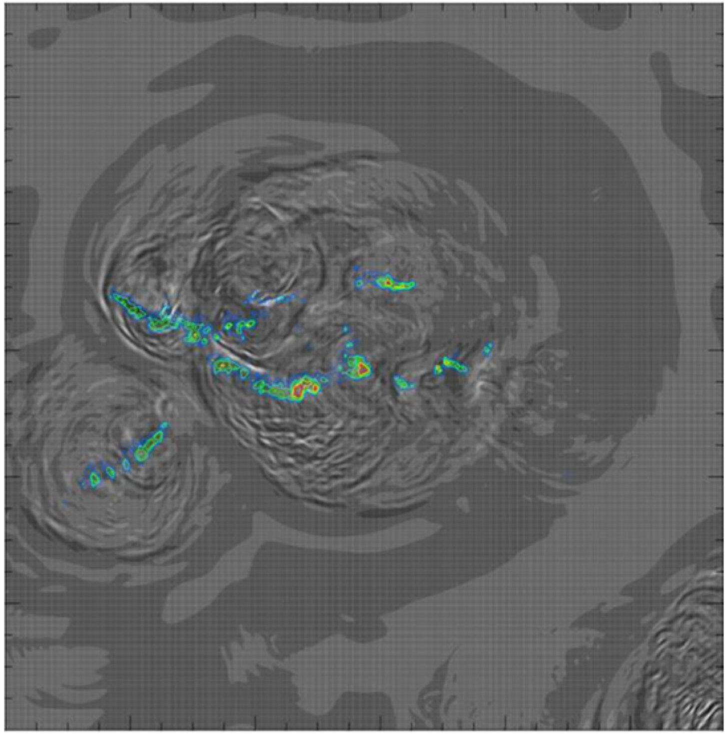

Radar observed rain (colors) and vertical velocities near the tropopause (gray shading).

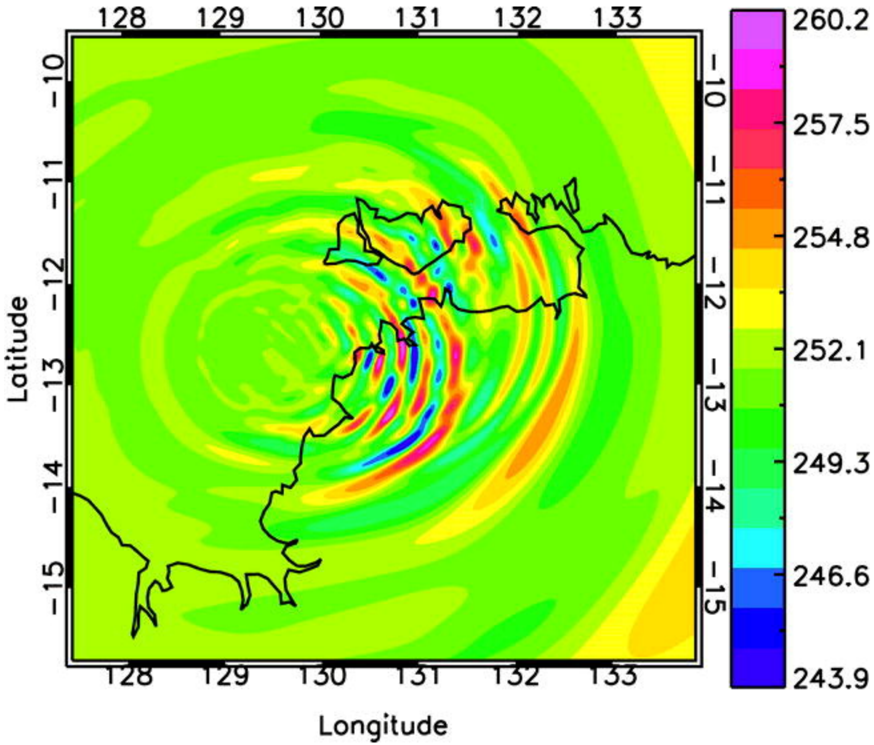

Simulated temperature at ~40 km altitude at the Australian coast.

Temperature responses to CO_2 increases in 1D RCE models

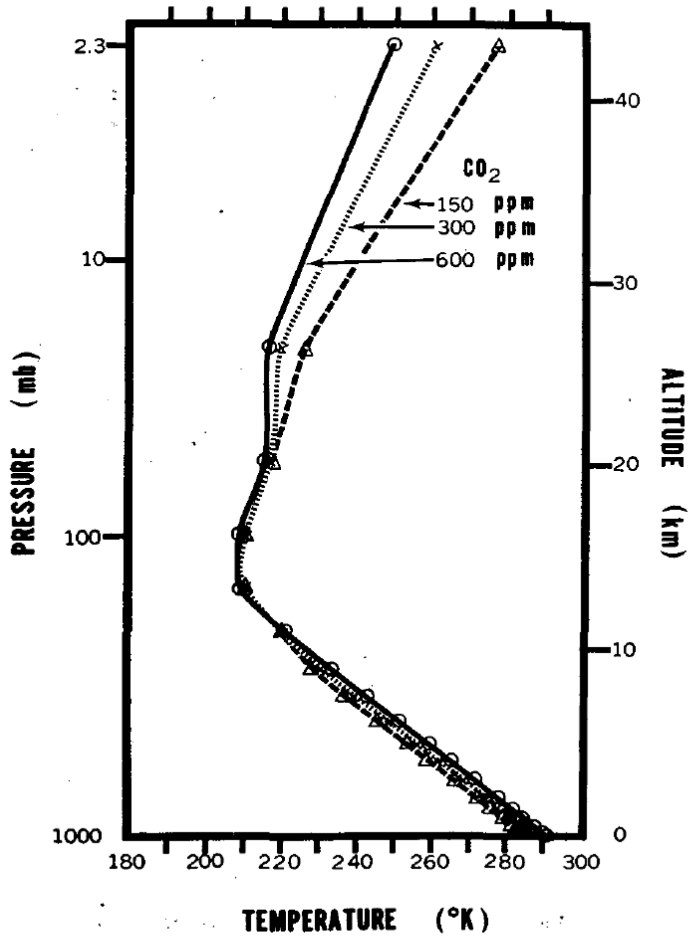

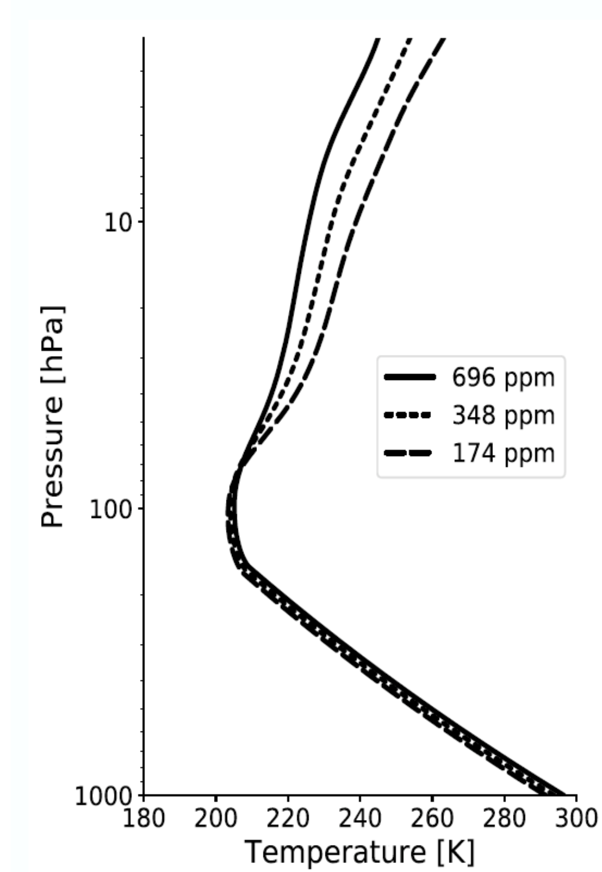

Manabe & Wetherald (1967) calculated a warming of 2.7 K for a doubling of CO2, Kluft et al., a warming of 2.8K.

Dependence of TTL temperatures on surface temperature in the 1D RCE model "konrad"

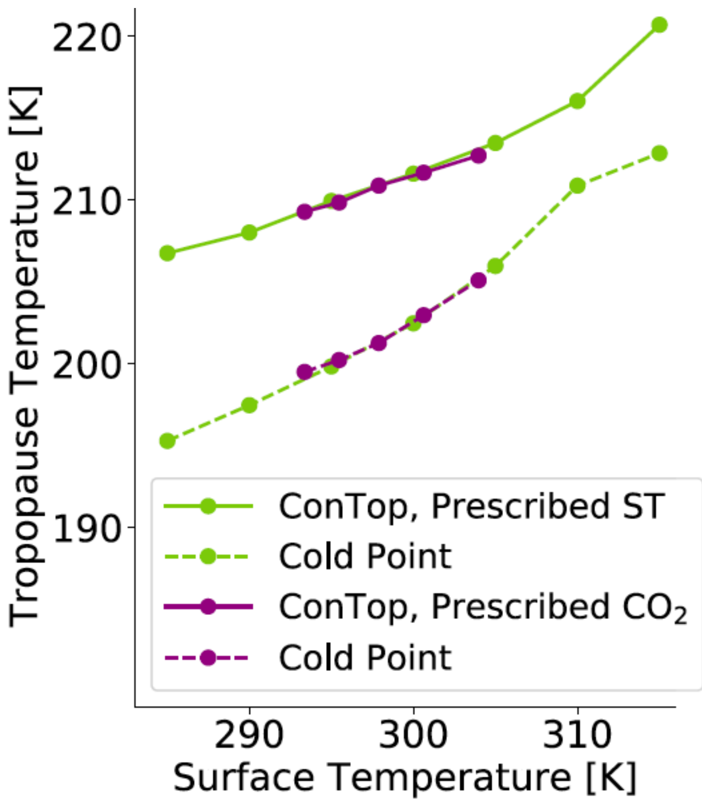

Assumptions in these simulations:

- O_3 profile constant in time
- Relative humidity fixed in troposphere, stratospheric H_2O vmr set by cold point temperature
- no mean upwelling

Effects of artificially shifted ozone profiles in the 1D RCE model "Konrad"

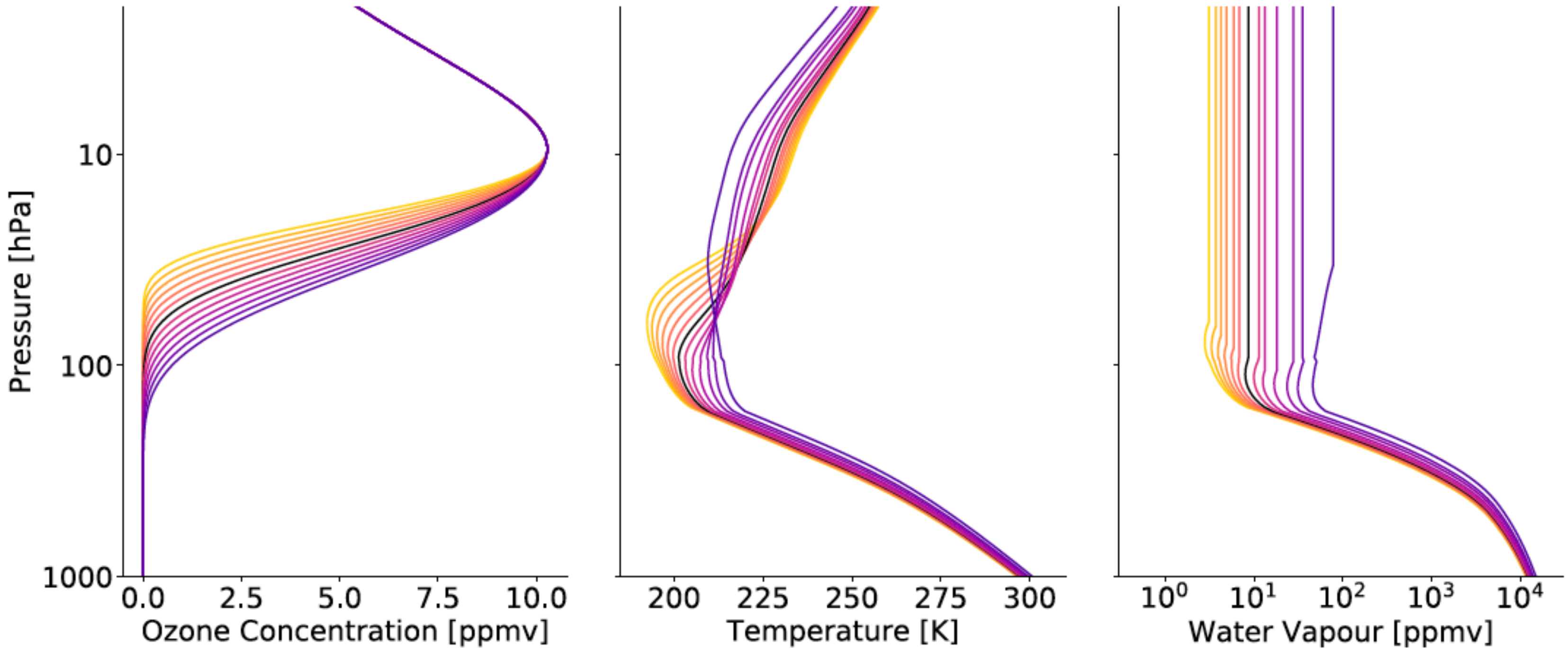

These are idealized ozone profile shifts. However, in $4xCO_2$ simulations where a profile shift from a complex model is prescribed the increase of the cold point temperature decreases from ~7K to ~5K.

Effects of different upwelling velocities at the tropopause in the 1D RCE model “Konrad”

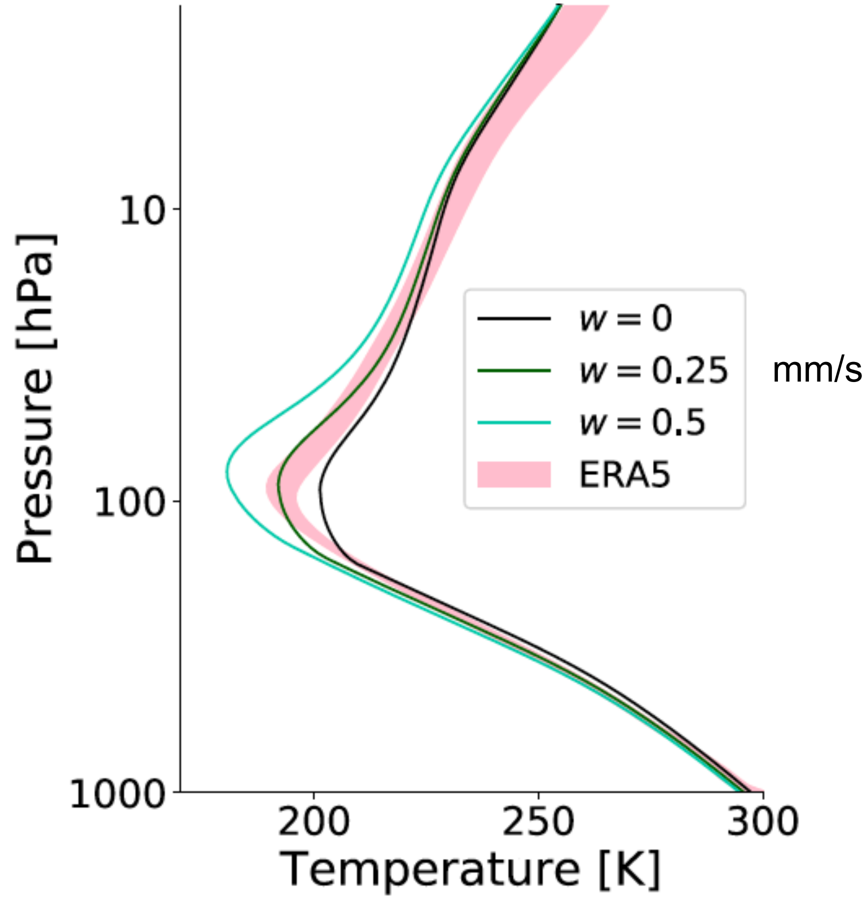

Trends in tropical tropospheric stability

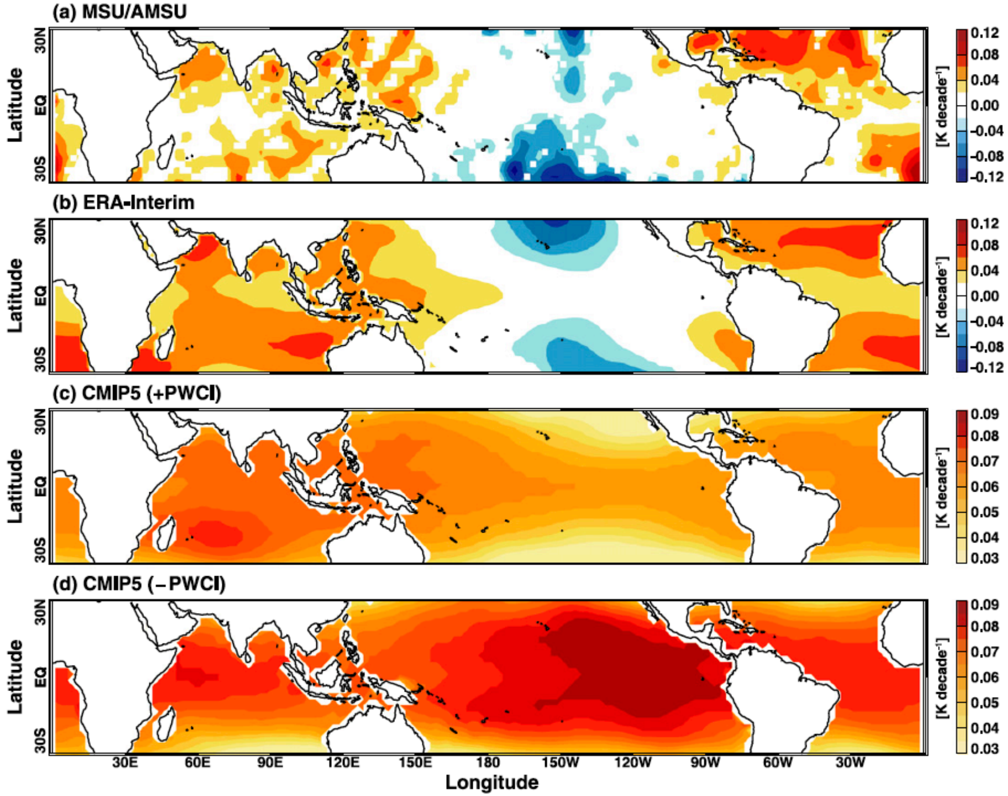

FIG. 3. Trend of the atmospheric component of the T24 − TLT trend over the 1979–2012 period from (a) MSU/AMSU, (b) ERAI, (c) CMIP5 +PWCI model, and (d) CMIP5 −PWCI model data. Only the areas exceeding the 90% confidence level are plotted in color.

(Sohn et al., J. Climate, 2016)

Max-Planck-Institut für Meteorologie

Walker circulation trends

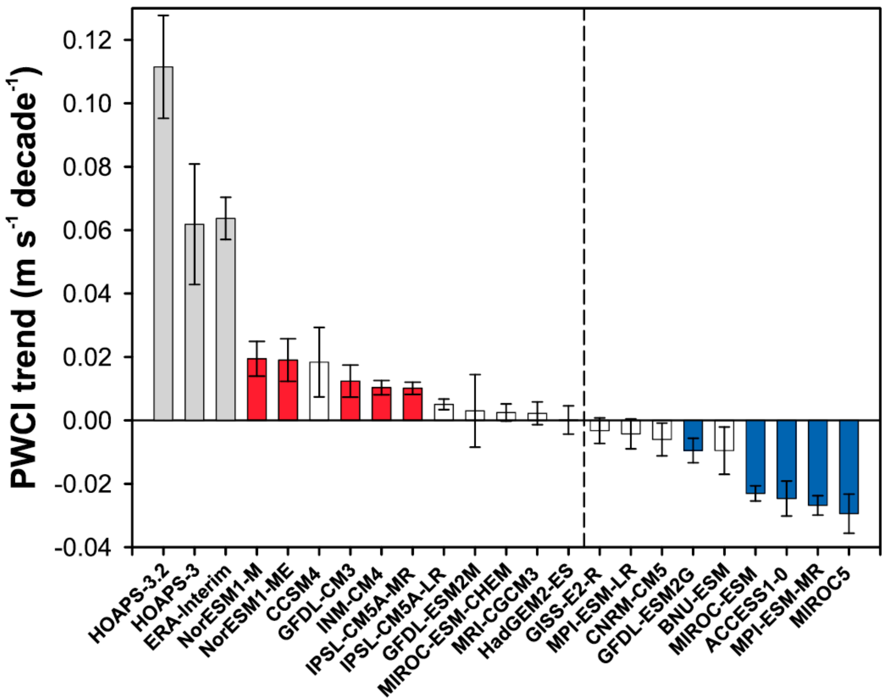

FIG. 2. Linear trend of PWCI calculated over the tropical Pacific domain (10°S–10°N, 120°E–120°W) using the HOAPS-3.2, HOAPS-3 SSM/I (Andersson et al. 2010), ERAI, and CMIP5 model data. Error bars denote the standard error of linear trends. CMIP5 models satisfying the 95% confidence level are highlighted in red (+PWCI) and blue (−PWCI).

The PWCI (Pacific Walker Circulation Index) is based on the strength of easterlies in the lower WC branch.

All trends are for the period 1979-2012, except HOAPS (1987-2008).

(Sohn et al., J. Climate, 2016)

SST trends in the tropical Pacific

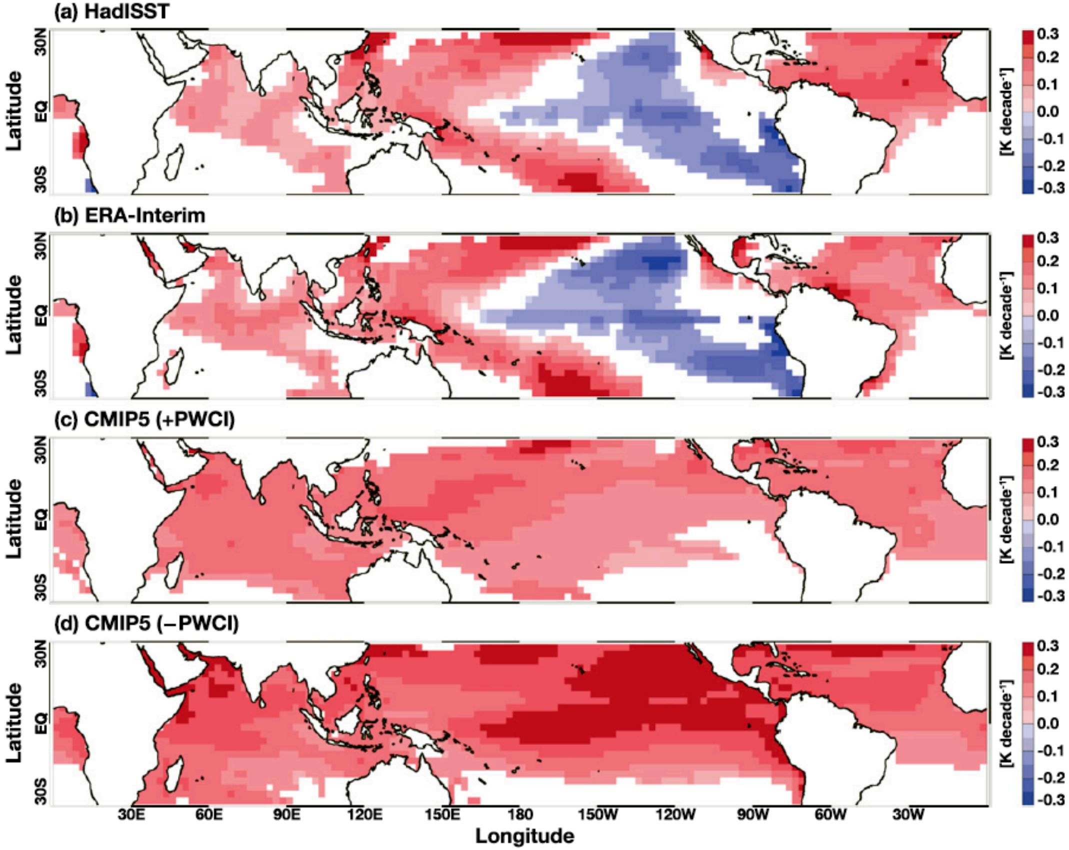

FIG. 6. Linear trend of SST from (a) HadISST, (b) ERAI, (c) CMIP5 +PWCI model, and (d) CMIP5 −PWCI model data for the period 1979–2012. The colors show the regions exceeding the 90% confidence level.

All trends are for the period 1979-2012.

Trends in tropical tropospheric stability

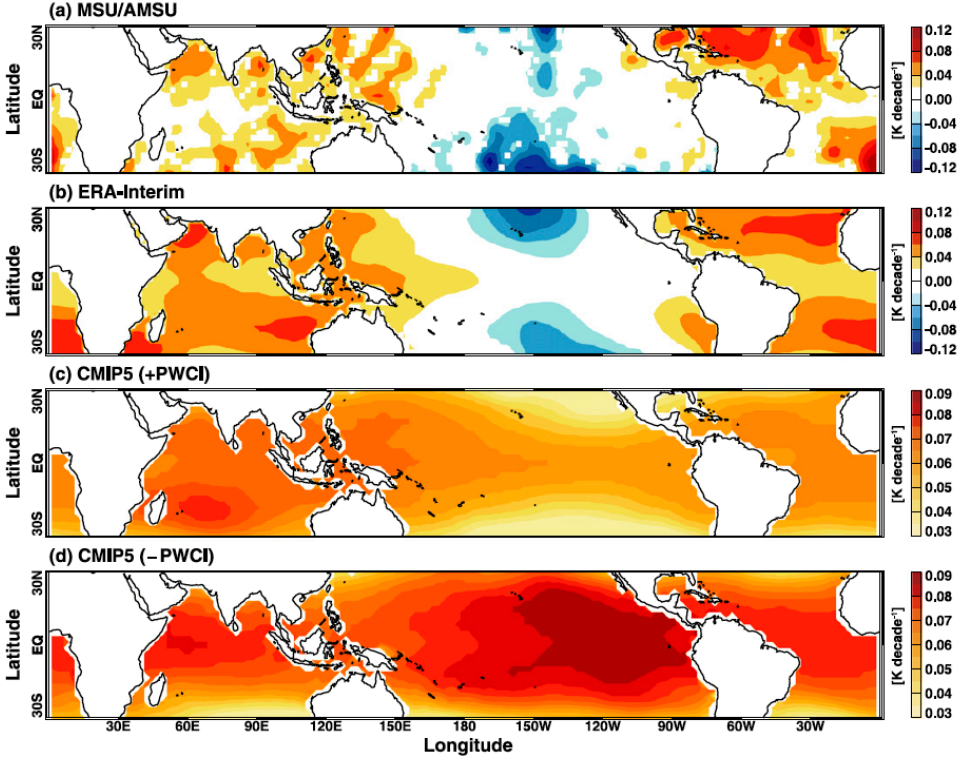

FIG. 3. Trend of the atmospheric component of the T24 − TLT trend over the 1979–2012 period from (a) MSU/AMSU, (b) ERAI, (c) CMIP5 +PWCI model, and (d) CMIP5 −PWCI model data. Only the areas exceeding the 90% confidence level are plotted in color.

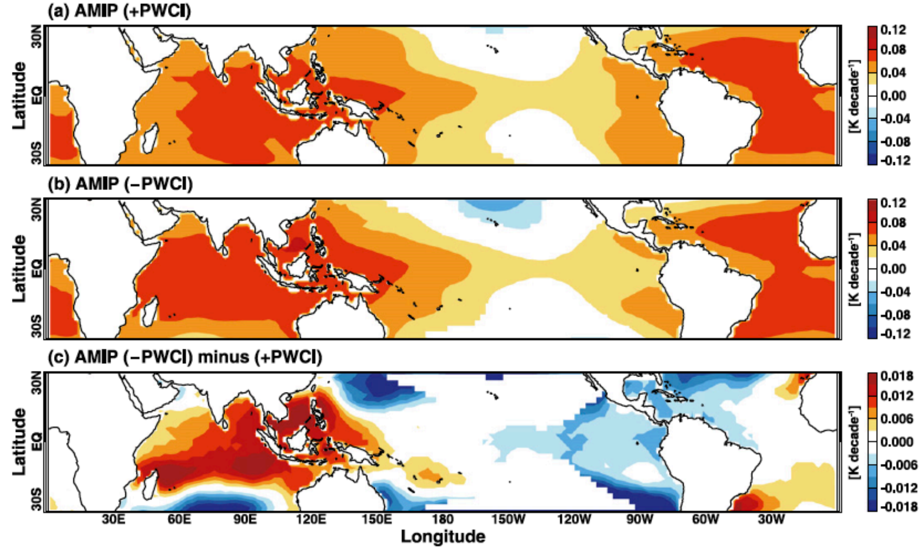

FIG. 7. Trend of the atmospheric component of the T24 − TLT trend over the 1979–2012 period from (a) AMIP +PWCI model, (b) AMIP −PWCI model data, and (c) AMIP −PWCI minus AMIP +PWCI model. Only the areas exceeding the 90% confidence level are plotted in color.

(Sohn et al., J. Climate, 2016)

Model projections of zonal mean tropospheric temperature change

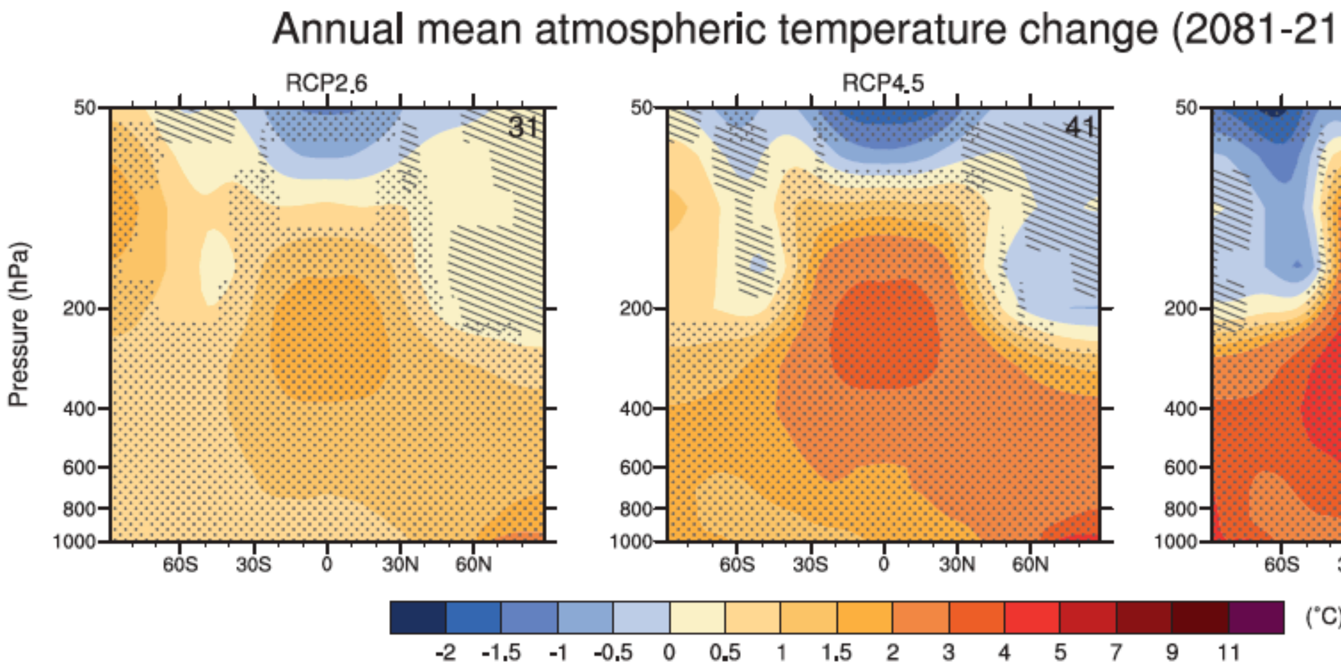

Figure 12.12 | CMIP5 multi-model changes in annual mean zonal mean temperature in the atmosphere and ocean relative to 1986–2005 for 2081–2100 under the RCP2.6 (left), RCP4.5 (centre) and RCP8.5 (right) forcing scenarios. Hatching indicates regions where the multi-model mean change is less than one standard deviation of internal variability. Stippling indicates regions where the multi-model change mean is greater than two standard deviations of internal variability and where at least 90% of the models agree on the sign of change (see Box 12.1).

(IPCC AR5, WG1, Fig. 12.12, Flato et al., 2013)

Response of T(k) and u (m/s) to idealized upper tropospheric heating

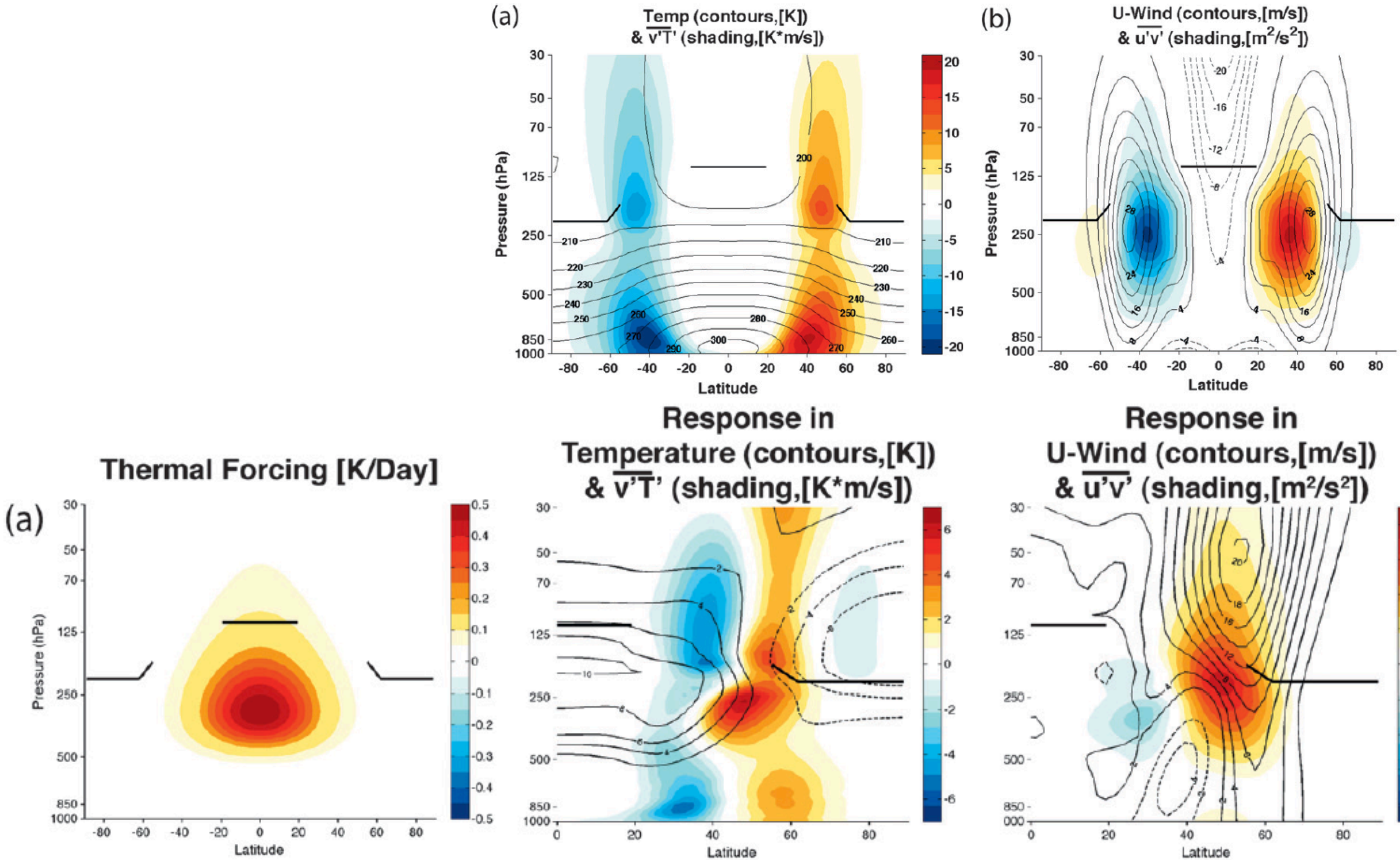

(Butler et al., J. Climate, 2010)

Deviations from a moist lapse rate in radiosonde observations and CMIP5 models

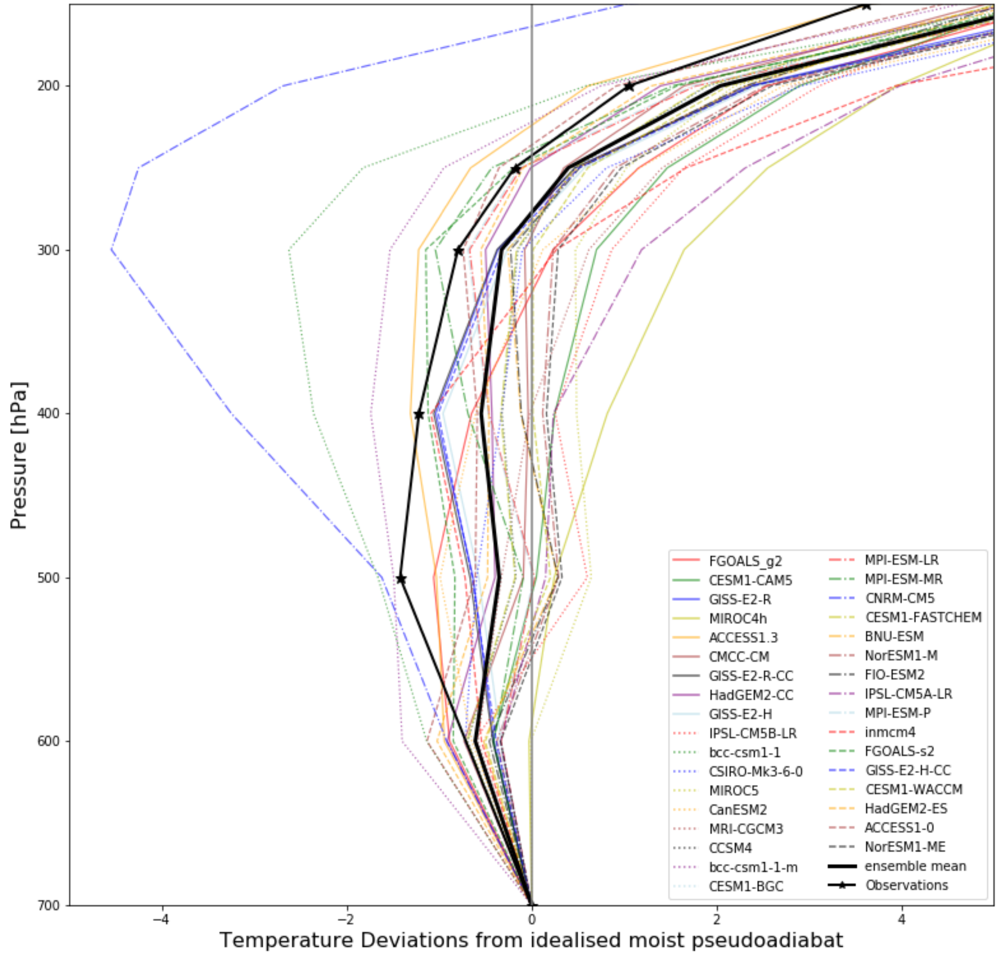

(Figure courtesy from Paul Keil)